# Statistical Analysis of Drift Wave Turbulence by the model with a Few Degrees of Freedom

Hamada, Daichi
Interdisciplinary Graduate School of Engineering Sciences, Kyushu University

Ito, Sanae-I.
Research Institute for Applied Mechanics, Kyushu University

Yagi, Masatoshi
Research Institute for Applied Mechanics, Kyushu University

Mori, Hazime
Research Institute for Applied Mechanics, Kyushu University

他

https://doi.org/10.15017/26833

出版情報：九州大学応用力学研究所所報. 133, pp.55-70, 2007-09. Research Institute for Applied Mechanics, Kyushu University
バージョン：

# Statistical Analysis of Drift Wave Turbulence by the model with a Few Degrees of Freedom

Daichi HAMADA*1, Sanae-I. ITOH *2, Masatoshi YAGI*2,
Hazime MORI*2 and Masafumi AZUMI*3
E-mail of corresponding author: *daichi@riam.kyushu-u.ac.jp*

( Received April 16, 2007 )

**Abstract**

The drift wave chaos is investigated using VZSC model [A. A. Vasil'ev, G. M. Zaslavsky, R. Z. Sagdeev, and A. A. Chernikov, Sov. J. Plasma Phys. 16 681(1991)], which is the reduced model of Hasegawa-Wakatani equations with a few degrees of freedom. The statistical properties of chaotic orbits is analyzed using the time correlation function and the power spectrum. The non-Markovian linear stochastic equation for the VZSC model is derived, applying Mori's projection operator method. The applicability of this method is partially confirmed through the comparison with numerical calculation.

**Key words :** *Chaos, Turbulence, Mori's Projection Operator, Hasegawa-Wakatani Equations, Drift Wave, Lorentz Model, Power Spectrum, Correlation Function*

## 1. Introduction

To achieve thermonuclear condition in a tokamak, it is necessary to confine the plasma for a sufficient time. Confinement is limitted by thermal conduction and convection processes in addition to various radiative loss. In the absence of instabilities, the confinement of tokamak plasma is determined by Coulomb collisions, so called neoclassical transport. Unfortunately, the transport which occurs in now-going experiments does not agree with the values predicted by neoclassical theory. Especially, the thermal transport by electrons can be up to two orders of magnitude higher than predicted one. The observed excess transport is considered to be caused by the so-called anomalous transport driven by microinstabilities in a plasma[1], and therefore the understanding of anomalous transport is crucial issue for the development of thermonuclear fusion reactor, like International Thermonuclear Experimental Reactor(ITER). The microinstabilities excited in a plasma generate the fine scale plasma turbulence and some of them are expected to greatly enhance the particle and energy losses from a plasma. Therefore various kind of microinstabilities are being studied in details theoretically and numerically as candidates of anomalous transport and tested through the comparison with experimental results. In these theoretical studies of anomalous transport, they focus their research to the evaluation of transport and the understanding of its mechanism, but the basic character of plasma turbulence, such as the statistical information, has been rarely studied so far. However the understanding of statistical properties of plasma turbulence is important not only from the basic understanding of mechanism of anomalous transport but also from the contribution to the basic physics covering wide research fields.

In this thesis, we study the statistical properties of drift wave turbulence. For this purpose, we employ the Hasegawa-Wakatani model as the model equation to drive the collisional drift wave turbulence and we reduce this equation to the coupled equations for small numbers of variables. We show these coupled equations exhibit the chaotic nature. In principle, we need a very large number of modes in order to descrive a fully-turbulent scenario due to the drift waves. However we are mainly interested to investigate the onset of turbulences, that is the scenario where a small number of modes gets unstable and leads to a cascade of higher modes. Therefore it is significant for investigating the process of turbulence to use low-dimensional model.

The Lorenz model[13] is an example of such an approach to the problem; it demonstrates the sequence of bifurcations and the formation finally of a chaotic attractor. Such a method can also be applied to the study

*1 Interdisciplinary Graduate School of Engineering Sciences, Kyushu University
*2 Research Institute for Applied Mechanics, Kyushu University
*3 Center for Computational Science and Systems, Japan Atomic Energy Agency

of the appearance of chaotic dynamics under the conditions of a collisional drift wave instability. This problem has, however, important differences from the problem of thermal convection discussed by Lorenz[13]. The finite-dimensional approximation can effectively be reduced to a set of four equations (there are three in the Lorenz model) so that the structure of the chaotic attractor also differs from the structure of the Lorenz attractor. Then we apply the Mori's statistical theory to these equations and clarify the statistical characters of the drift wave turbulence of Hasegawa-Wakatani model in detail.

This thesis is organized as follows. In Chapter 2, we review the chaotic model of collisional drift wave, reduced from Hasegawa-Wakatani model with a few degrees of freedom, and describe the Mori's projection operator method which is an analytical technique for chaos and turbulence. In Chapter 3, we perform the numerical simulation using the model equation and analyze simulation results. We show the successive transition from the limit cycle to the chaos by changing the parameter. In Chapter 4, we derive the non-Markovian linear stochastic equation for the model equation, and compare numerical results with the direct numerical results in Chapter 3. Finally, in Chapter 5, summery and discussions are given.

## 2. Reviews

In this chapter, we derive the chaotic model for the collisional drift wave with a few degrees of freedom starting from Hasegawa-Wakatani model. Then, the Mori's projection operator method which is an analytical technique for chaos and turbulence is briefly explained.

### 2.1 Derivation of the model equation

#### 2.1.1 Hasegawa-Wakatani model

Hasegawa-Wakatani (HW) model describes the nonlinear dynamics for the collisional drift-wave turbulence in a magnetized plasma[4]. It consists of the vortisity equation and the continuity equation which describe the nonlinear evolution of the potential $\phi$ and density fluctuation $n$ in a spatially inhomogeneous plasma. We consider the Cartesian coodinate $(x, y, z)$ where the mean density gradient $dn_0/dx$ is in the $x$ direction and magnetic field in the $z$ direction. In dimensionless units, the model equations are written by

$$\begin{aligned} &\frac{\partial}{\partial t}\nabla_\perp^2\phi + [\phi, \nabla_\perp^2\phi] = -\hat{C}\frac{\partial^2}{\partial z^2}(\phi - n) + \mu\nabla_\perp^4 n, \\ &\frac{\partial}{\partial t}n + [\phi, n] + \kappa\frac{\partial \phi}{\partial y} = -\hat{C}\frac{\partial^2}{\partial z^2}(\phi - n) + D\nabla_\perp^2 n, \end{aligned} \tag{1}$$

where

$$[a, b] \equiv \boldsymbol{z}\cdot(\nabla a \times \nabla b),$$

is the Poisson bracket which implies the convective derivative, and

$$D = \frac{2\nu_{ei||}m_e}{m_i}, \qquad \hat{C} = \frac{2}{D}, \qquad \kappa = \boldsymbol{z}\times\nabla\ln n_0.$$

In Eq.(1) the following normalization is used:

$$\Omega_i t \to t, \quad \frac{r}{\rho_s} \to r, \quad \frac{n}{n_0} \to n, \quad \frac{e\phi}{T_{e0}} \to \phi, \quad \frac{\nu_{ei}}{\Omega_i} \to \nu_{ei}. \tag{2}$$

Here $T_{e0}$ is electron temperature, $\Omega_i$ is the ion cyclotron frequency, and $\nu_{ei}$ is the effective electron-ion collision frequency, the subscripts "$e, i$" indicate electrons and ions respectively. If we set $\nu_{ei}$ and $\mu$ equal to zero in Eq.(1) then, it reduced to the well known Charney-Hasegawa-Mima (HM) equation[5] used in geophysics and plasma physics.

Linearizing Eq.(1), we have

$$\begin{aligned} -i\omega(-k_\perp^2\phi) &= \hat{C}k_z^2(\phi - n) + \mu k_\perp^4\phi, \\ -i\omega n - ik_y\kappa\phi &= \hat{C}k_z^2(\phi - n) - Dk_\perp^2 n. \end{aligned} \tag{3}$$

Then the dispersion relation is obtained by

$$\begin{aligned} &\omega^2 + i\omega\left(\hat{C}k_z^2 + Dk_\perp^2 + \hat{C}\frac{k_z^2}{k_\perp^2} + \mu k_\perp^2\right) + \frac{ik_y\kappa k_z\hat{C}}{k_\perp^2} \\ &- \left(\hat{C}^2\frac{k_z^4}{k_\perp^2} + \hat{C}Dk_z^2 - \mu\hat{C}k_\perp^2k_z^2 - \mu Dk_\perp^4 - \hat{C}^2\frac{k_z^3}{k_\perp^2}\right) = 0. \end{aligned} \tag{4}$$

#### 2.1.2 Vasil'ev-Zaslavsky-Sagdeev-Chernikov model

In order to derivate the chaotic model with a few degrees of freedom, we apply the Galerkin approximation method to Eq.(1)[2]. We expand $\phi$ and $n$ as

$$\phi = \phi_1(x, y, t)\cos(k_z z) + \phi_2(x, y, t)\cos(2k_z z), \tag{5}$$

$$n = n_1(x, y, t)\cos(k_z z) + n_2(x, y, t)\cos(2k_z z), \tag{6}$$

with

$$\phi_{1,2} = \sum_{m,n} A_{m,n}^{(1,2)}(t)\sin(mk_x x)\cos(nk_y y), \tag{7}$$

where the index $m$, $n$ indicate a set of integer values while the amplitudes $A_{mn}^{(i)}$ depend only on the time. We neglect higher harmonics and keep only seven harmonics

$$A_{m,n}^{(i)} = \{A_{10}^{(1)}, A_{11}^{(1)}, A_{20}^{(1)}, A_{21}^{(1)}, A_{10}^{(2)}, A_{11}^{(2)}, A_{20}^{(2)}\}. \tag{8}$$

Numerical simulation of the corresponding system shows that amplitudes $A_{10}^{(1)}$, $A_{20}^{(1)}$, and $A_{21}^{(2)}$ decay rapidly with time and only four amplitudes in Eq.(8) survive,

$$\begin{aligned} \phi_1 = \{&A_{11}^{(1)}(t)\sin(k_x x) + A_{21}^{(1)}(t)\sin(2k_x x)\} \\ &\times\cos(k_y y - \kappa k_y t), \end{aligned} \tag{9}$$

$$\phi_2 = A_{10}^{(2)}(t)\sin(k_x x) + A_{20}^{(2)}(t)\sin(2k_x x). \tag{10}$$

Neglecting $[\phi, \nabla_\perp^2 \phi]$ nonlinearity in Eq.(1), we obtain

$$n_1 = \phi_1 - \frac{1}{\hat{C}k_z^2}\frac{\partial}{\partial t}\nabla_\perp^2\phi_1 + \frac{\mu}{\hat{C}k_z^2}\nabla_\perp^4\phi_1, \tag{11}$$

$$n_2 = \phi_2 - \frac{1}{4\hat{C}k_z^2}\frac{\partial}{\partial t}\nabla_\perp^2\phi_2 + \frac{\mu}{4\hat{C}k_z^2}\nabla_\perp^4\phi_2. \tag{12}$$

Substituting Eqs.(9)-(12) into Eqs.(1), HW model reduces to Vasil'ev-Zaslavsky-Sagdeev-Chernikov model (VZSC model)[2)]

$$\begin{aligned}
\frac{dX}{dt} &= \nu(R-1)X - \frac{1}{2}fUZ + XY,\\
\frac{dU}{dt} &= \nu f(R-f)U - \frac{1}{2}XZ,\\
\frac{dZ}{dt} &= -\frac{e}{16}Z + \frac{1}{4}(1+f)UX,\\
\frac{dY}{dt} &= -eY - \frac{1}{2}X^2,
\end{aligned} \tag{13}$$

where

$$\begin{aligned}
k_{1\perp}^2 = k_x^2 + k_y^2, f = 1 + \frac{3k_x^2}{k_{1\perp}^2}, e = \frac{16\nu k_x^4}{k_\perp^4},\\
\nu = \mu k_{1\perp}^4, X = \frac{A_{11}^{(1)}}{d}, U = \frac{A_{21}^{(1)}}{d},\\
Z = \frac{A_{10}^{(2)}}{d}, Y = \frac{A_{20}^{(2)}}{d},\\
d = \frac{2Ck_z^2}{\kappa k_x k_y^2 k_{1\perp}^2}, R = \frac{\kappa^2 k_y^2}{Ck_z^2\mu k_{1\perp}^2}.
\end{aligned} \tag{14}$$

Using Eq.(13), the dimensionless potential $\phi$ is given by

$$\begin{aligned}
\phi &= d\{X\sin(k_x x) + U\sin(2k_x x)\}\cos(k_y y - \kappa k_y t)\cos k_z z\\
&+ d\{Z\sin(k_x x) + Y\sin(2k_x x)\}\cos(2k_z z).
\end{aligned} \tag{15}$$

It should be noticed that $\omega^* = \kappa k_y$ in this normalization, therefore the drift wave is described by the term proportional to $\cos(k_y y - \kappa k_y t)$.

### 2.1.3 Fixed point of the VZSC model

To investigate bifurcations in the four-dimensional phase space of VZSC model, we calculate fixed point. Setting $d/dt = 0$, we have

$$\nu(R-1)X - \frac{1}{2}fUZ + XY = 0, \tag{16}$$

$$\nu f(R-f)U - \frac{1}{2}XZ = 0, \tag{17}$$

$$-\frac{e}{16}Z + \frac{1}{4}(1+f)UX = 0, \tag{18}$$

$$-eY - \frac{1}{2}X^2 = 0. \tag{19}$$

From Eq.(17),

$$U = \frac{1}{2\nu f(R-f)}XZ. \tag{20}$$

Substituting Eq.(20) into Eq.(18), then we obtain two solutions:

$$Z = 0, \tag{21}$$

or

$$X = \pm\sqrt{\frac{e\nu f(R-f)}{2(1+f)}}. \tag{22}$$

If $Z = 0$ holds, then $X = 0$ or $U = 0$ from Eq.(20). In the case of $X = Z = 0$, the first fixed point is given by

$$X_0 = U_0 = Z_0 = Y_0 = 0. \tag{23}$$

In the case of $Z = U = 0$, the second fixed point is given by

$$X_0 = \pm\sqrt{2e\nu(R-1)}, \quad Y_0 = -\nu(R-1), \quad U_0 = Z_0 = 0. \tag{24}$$

If (22) holds, then the third fixed point is obtained as

$$\begin{aligned}
X_0 = \pm\sqrt{\frac{e\nu f(R-f)}{2(1+f)}}, \quad Y_0 = -\frac{\nu f(R-f)}{4(1+f)},\\
U_0 = \pm\sqrt{\frac{\nu e}{2f(1+f)}\left(R - 1 - \frac{f(R-f)}{4(1+f)}\right)},\\
Z_0 = 2\nu\sqrt{(R-f)\left(R - 1 - \frac{f(R-f)}{4(1+f)}\right)}.
\end{aligned} \tag{25}$$

Next, we analyze the stability around the fixed point. Linearizing Eq.(23) around the fixed point, the eigenvalue equation is given by

$$\lambda\begin{pmatrix}\delta X\\ \delta U\\ \delta Z\\ \delta Y\end{pmatrix} = \begin{pmatrix} Y_0 + \nu(R-1) & -fZ_0/2 & -fU_0/2 & X_0\\ -Z_0/2 & \nu f(R-f) & -X_0/2 & 0\\ (1+f)U_0/4 & (1+f)X_0/4 & -e/16 & 0\\ -X_0 & 0 & 0 & -e\end{pmatrix} \times \begin{pmatrix}\delta X\\ \delta U\\ \delta Z\\ \delta Y\end{pmatrix}, \tag{26}$$

where $\lambda$ represents the eigenvalue. For Eq.(23), we have

$$\lambda = -e, -e/16, \nu(R-1), \nu f(R-f). \tag{27}$$

For Eq.(24), we have

$$\lambda = \frac{-e \pm \sqrt{e^2 - 8e\nu(R-1)}}{2}, \tag{28}$$

and

$$\lambda = \frac{\epsilon \pm \sqrt{(\epsilon + e/8)^2 - (1+f)X_0^2/2}}{2}, \tag{29}$$

where

$$\epsilon = \nu f(R-f) - \frac{e}{16}. \tag{30}$$

It is clear that for $\epsilon < 0$, the fixed point is stable. It is easily shown that for $\epsilon = 0$, the value in the square root in (29) is negative. Thus, for $\epsilon = 0$, a pair of eigenvalues (29) passes through the imaginary axis and a Poincaré-Andronov-Hopf bifurcation[15)] occurs. From (30), the critical value $R_c$ is given by

$$R_c = \frac{e}{16f\nu} + f. \tag{31}$$

For $f = 1.795, \nu = 1.06775, e = 1.2$, the critical value is estimated as $R_c = 1.834131\ldots$. the fixed point loses its stability and a stable limit cycle appears. When the parameter $\epsilon$ increases the amplitude of limit cycle increases. We assume the first bifurcation occurs at $\epsilon = \epsilon_1$, and for $\epsilon = \epsilon_2$ the first period doubling bifurcation occurs, and as $\epsilon$ increases further each of the cycles passes through a sequence of period doubling bifurcations at $\epsilon = \epsilon_3, \epsilon_4 \ldots$. The doubling constant

$$\delta = \lim_{n\to\infty} \frac{\epsilon_{n+1} - \epsilon_n}{\epsilon_n - \epsilon_{n-1}} \approx 4.66\ldots \qquad (32)$$

was numerically found to be close to Feigenbaum's universal constant[16].

## 2.2 The Mori's projection operator method

### 2.2.1 Derivation of stochastic equation

The Mori's projection operator technique[6] is a method for deriving the generalized Langevin equation from Newton equation by means of the projection operator. Let us denote their state variables in phase space by $X(t) = \{X_j(t)\}$ $(j = 1, 2, \ldots, d)$, where $d$ is the number of degrees of freedom. The fluctuations of the macrovariables $A(t)$ are evoluved as

$$\frac{dA(t)}{dt} = \Lambda \exp(t\Lambda)A = \Lambda A(t), \qquad (33)$$

where we assume $\langle A(t)\rangle = 0$, and the we defined the Liouville operator is given by

$$\Lambda \equiv \sum_{j=1}^{d} \dot{X}_j \frac{\partial}{\partial X_j}. \qquad (34)$$

Here the relation holds as

$$A(t) = \exp(t\Lambda)A, \qquad (35)$$

where $X_j = X_j(t=0), A = A(t=0)$. Let us define the inner product of two functions $f_1(t)$ and $f_2(0)$ by the long-time average over a chaotic orbit $X(s)$,

$$\langle f_1(t) f_2(0)\rangle \equiv \lim_{\tau\to\infty} \frac{1}{\tau}\int_0^{\tau} ds\ f_1(t+s) f_2(s), \qquad (36)$$

Projection operator $\mathcal{P}$ is defined by

$$\mathcal{P}G(A(t)) = \langle G(A(t))A^\dagger\rangle \langle AA^\dagger\rangle^{-1} A, \qquad (37)$$

where $\mathcal{P}$ is the projection of a quantity $G(A(t))$ onto the macrovariables $A = A(t=0)$. Using projection operator, $A(t)$ is derived into two parts:

$$\begin{aligned} A(t) &= \mathcal{P}A(t) + \mathcal{Q}A(t) = \langle A(t)A^\dagger\rangle\langle AA^\dagger\rangle^{-1}A + \mathcal{Q}A(t), \\ &= \Xi(t)A + A'(t), \end{aligned} \qquad (38)$$

where

$$\Xi(t) \equiv \langle A(t)A^\dagger\rangle\langle AA^\dagger\rangle^{-1} \qquad (39)$$

$$\mathcal{Q} \equiv 1 - \mathcal{P}, \quad A'(t) \equiv \mathcal{Q}A(t). \qquad (40)$$

$A(t)$ denotes the fluctuations around its mean value and $\Xi(t)$ represents the most probable path. In order to determine the fluctuations $A'(t)$, let us multiply (33) by $\mathcal{Q}$ from the left and insert (38) into $A(t)$ on the right-hand side, we obtain

$$\begin{aligned} \frac{dA'(t)}{dt} &= \mathcal{Q}\frac{dA(t)}{dt} = \mathcal{Q}\Lambda A(t), \\ &= \mathcal{Q}\Lambda(\mathcal{P}+\mathcal{Q})A(t), \\ &= \mathcal{Q}\Lambda(A'(t) + \Xi(t)A). \end{aligned} \qquad (41)$$

Using $A'(t=0) = 0$, this is integrated to give

$$A'(t) = \int_0^t ds\ \Xi(s)\widetilde{R}(t-s), \qquad (42)$$

where

$$\widetilde{R}(t) \equiv \exp(t\mathcal{Q}\Lambda)\mathcal{Q}\dot{A}. \qquad (43)$$

$\widetilde{R}(t)$ gives the most probable nonlinear force with $\dot{A} = \Lambda A$.

$$A(t) = \Xi(t)A + \int_0^t ds\ \Xi(t-s)\widetilde{R}(s). \qquad (44)$$

The first part of Eq.(44) represents the most probable path $\mathcal{P}A(t)$, and the second part consists of the fluctuations $\mathcal{Q}A(t)$ around it. The orthogonality of the two parts is ensured by the operator $\mathcal{Q}$ of the unnatural propagator of (43).

Since $A(t) = e^{t\Lambda}A$, the evolution equation can be written as

$$\frac{dA(t)}{dt} = e^{t\Lambda}(\mathcal{P}+\mathcal{Q})\dot{A} = i\Omega A(t) + e^{t\Lambda}\mathcal{Q}\dot{A}, \qquad (45)$$

where we have defined the square matrix

$$i\Omega \equiv \langle \dot{A}A^\dagger\rangle\langle AA^\dagger\rangle^{-1}. \qquad (46)$$

which is a frequency matrix if $\dot{A}$ is invariant under time reversal. Substituting the operator identity (see Appendix A.1)

$$e^{t\Lambda} = e^{t\mathcal{Q}\Lambda} + \int_0^t ds\ e^{(t-s)\Lambda}\mathcal{P}\Lambda e^{s\mathcal{Q}\Lambda} \qquad (47)$$

into Eq.(45), we obtain

$$\frac{d}{dt}A(t) = i\Omega A(t) - \int_0^t ds\ \mathcal{M}(s)A(t-s) + \widetilde{R}(t), \qquad (48)$$

where the memory function is defined by

$$\mathcal{M}(t) \equiv -\langle \Lambda\widetilde{R}(t)A^\dagger\rangle\langle AA^\dagger\rangle^{-1} = \langle \widetilde{R}(t)\widetilde{R}^\dagger\rangle\langle AA^\dagger\rangle^{-1}. \qquad (49)$$

To derive Eq.(49), we used the identity $\langle \Lambda R(t)A^\dagger\rangle = -\langle R(t)R^\dagger\rangle$ (see Appendix A.2). Eq.(48) is the generalized Langevin equation. Using the relation $\langle \widetilde{R}(t)A^\dagger\rangle = 0$, the evolution of most probable path is given by

$$\frac{d}{dt}\Xi(t) - i\Omega\Xi(t) + \int_0^t ds\ \mathcal{M}(s)\Xi(t-s) = 0. \qquad (50)$$

The formal solution of this equation can be found by Laplace transform. The result is

$$\Xi(z) \equiv \int_0^t dt\, e^{-zt}\Xi(t) = \frac{1}{z - i\Omega + \mathcal{M}(z)}, \quad (51)$$

where $\mathcal{M}(z)$ is the Laplace transform of the memory function (49). Thus it turns out that the projection operator method just extracts the linear long-lived motion (50) from the evolution equation (33).

The time evolution of the memory function (49) is governed by the unnatural propagator $\exp(t\mathcal{Q}\Lambda)$ of (43), where the projection operator $\mathcal{Q}$ excludes the nonlinear long-lived motion (50), so that the memory function $\mathcal{M}(t)$ does not include the linear long-lived motion $\Xi(t)$. Therefore, the fluctuating force $\widetilde{R}(t)$ consists of nonlinear terms of $A(t)$ and coupling terms of $A(t)$, both of which usually change much faster than the linear long-lived motion $\Xi(t)$. This indicates that the memory function $\mathcal{M}(t)$ usually consists of short-lived motion with a short timescale $\tau_r$. Therefore $\mathcal{M}(t)$ is given by

$$\mathcal{M}(t) = 2\Gamma\delta(t) \quad (52)$$

on a long timescale $\tau_M(\gg \tau_r)$, where $\delta(t)$ is the $\delta$-function. Then (50) becomes Markovian, leading to

$$\Xi(t) = \exp[(i\Omega - \Gamma)t], \quad (53)$$

which represents the linear long-lived motion with long timescale $\tau_M \sim 1/Tr\Gamma$, where $Tr\Gamma$ represents the trace of $\Gamma$.

In order to explore the short-lived motion of the memory function $\mathcal{M}(t)$, we defined the nonlinear force $\widetilde{F}(t)$

$$\widetilde{F}(t) \equiv e^{t\Lambda}\mathcal{Q}\dot{A} = \widetilde{R}(t) - \int_0^t ds\, \mathcal{M}(t-s)A(s). \quad (54)$$

Then time correlation of the nonlinear force $\widetilde{F}(t)$ is obtained by

$$\widetilde{\Phi}(t) = \mathcal{M}(t) - \int_0^t ds\, \mathcal{M}(t-s)\langle A(s)\widetilde{R}^{\dagger}\rangle\langle AA^{\dagger}\rangle^{-1}, \quad (55)$$

where the relation

$$\widetilde{\Phi}(t) \equiv \langle \widetilde{F}(t)\widetilde{F}\rangle\langle AA^{\dagger}\rangle^{-1}, \quad (56)$$

$$\widetilde{F}(t=0) = \widetilde{R}(t=0)$$

is used to derive Eq.(55). The Laplace transform of the above equation gives

$$\widetilde{\Phi}(z) = \mathcal{M}(z) - \mathcal{M}(z)\Xi(z)\mathcal{M}(z). \quad (57)$$

This is the relation between $\widetilde{\Phi}(t)$ and $\mathcal{M}(t)$. The second term on the right-hand side of Eq.(57) contains the linear long-time motion $\Xi(t)$.

### 2.2.2 Markovian approximation

Markovian approximation is based on the following two assumptions:

- The change of $A(t)$ is very slow, compared to the change of memory function.
- memory is lost for a long time scale.

Using the first assumption to Eq.(48)

$$\int_0^t ds\, \mathcal{M}(s)A(t-s) = \int_0^t ds\, \mathcal{M}(t-s)A(s) \simeq A(t)\int_0^t ds\, \mathcal{M}(t-s) \quad (58)$$

It indicates the change of $A(t)$ is much slower than $\mathcal{M}(t)$. Applying the second assumption, we get

$$-A(t)\int_0^{\infty} d\tau\, \mathcal{M}(\tau) = \gamma A(t) \quad (59)$$

where

$$\gamma \equiv -\int_0^{\infty} d\tau\, \mathcal{M}(\tau), \quad \tau = t - s \quad (60)$$

Finally, the generalized Langevin equation (48) is reduced to the Langevin equation giving by

$$\dot{A}(t) = (i\Omega - \gamma)A(t) + \widetilde{R}(t). \quad (61)$$

## 3. Direct numerical simulation of the VZSC model

### 3.1 Statistical Property of the VZSC model

In this chapter, we study the statistical properties of VZSC model (13) by using the DNS(direct numerical simulation). In order to solve Eq.(13), we use a fourth-order Runge-Kutta method with a time integration step $\Delta t = 0.001$. In this simulation, parameter $R$ is chosen as an order parameter to characterize the system behavior and the other parameters are fixed as

$$\nu = 1.06775,\ e = 1.2,\ f = 1.795. \quad (62)$$

Initial values are given by

$$(X, U, Z, Y) = (0.15,\ 0.001,\ 0.001, -0.05). \quad (63)$$

In order to understand the transitions of attractors, we calculate the Lyapunov exponents. Parameter $R$ is changed from 1.83 to 1.88. If the maximum Lyapunov exponent exists to be positive, then the system becomes chaotic. The periodic solution appears if the maximum Lyapunov exponent is zero. The solution converges to the fixed points, if all Lyapunov exponents are negative.

Figure.1 (a) shows the dependence of Lyapunov exponents on $R$. It is found that in the regime $R < 1.8344$, the fixed point exists and for $R \simeq 1.8344$, Lyapunov exponent is almost zero. In the regime $1.8344 \leq R \lesssim 1.8725$ the maximum Lyapunov exponent has a small

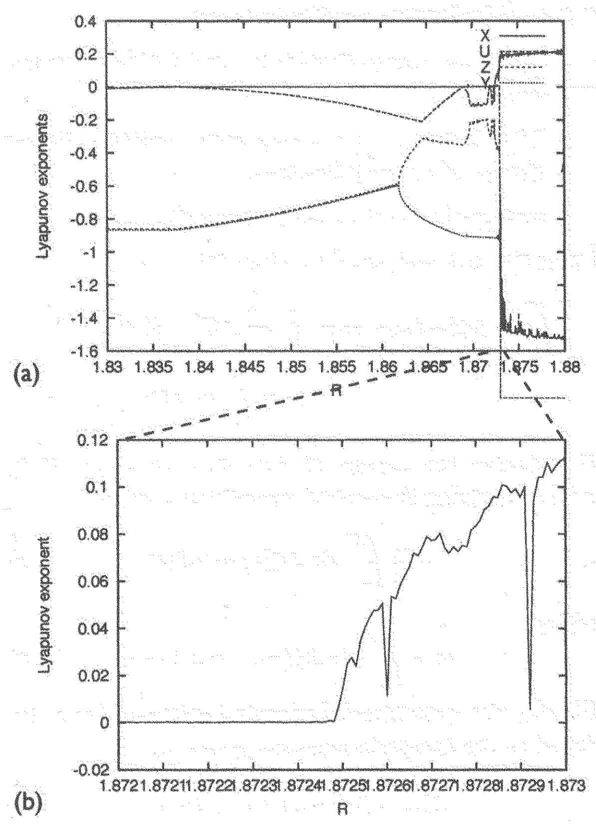


Fig. 1 (a)Dependece of Lyapunov exponents on $R$. (b)Extended view of Figure.1(a) around $R = 1.872$.

positive value. We found the chaotic attractor in the regime $1.8725 < R$ (extended view of Figure.1(a) around $R = 1.872$ is shown in Figure.1(b)).

## 3.2 Bifurcation in the set VZSC model

Figure.2 shows the bifurcation diagram of $X$ on $R$ in the range of $1.83 < R < 1.873$. In the regime $R > 1.873$, the result can not be obtained due to the numerical problem. It is found that the first bifurcation occurs at $R = 1.8346$. At $R = 1.8691$, the first period-doubling bifurcation occurs. The second period-doubling bifurcation occurs at $R = 1.8719$. Typical examples of the trajectory in the $X$-$Y$ phase space, the time evolution $X$ and the time correlation function of $X$, the power spectrum of $X$ for specific value of $R$ are shown in the next subsections.

### 3.2.1 Limit Cycle at $R = 1.8346$

At $R = 1.8346$, the maximum Lyapunov exponent is almost zero, so that the limit cycle is expected. Figure.3 shows the power spectrum of $X$. It is seen that the spectrum has one peak. Figure.4(a) shows the trajectory of the solutions in the $X$-$Y$ phase space. It

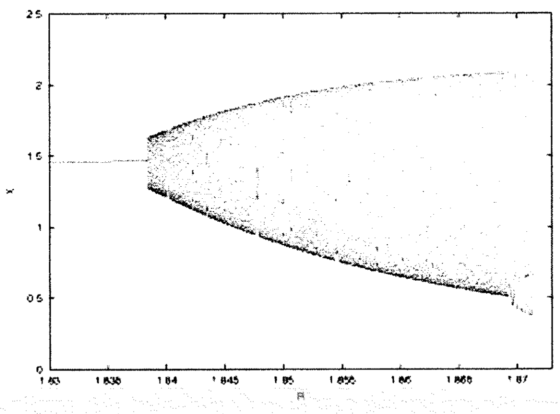


Fig. 2 Bifurcation diagram of $X$ on $R$.

shows the limit cycle solution. Figure.4(b) shows the time evolution of $X$.

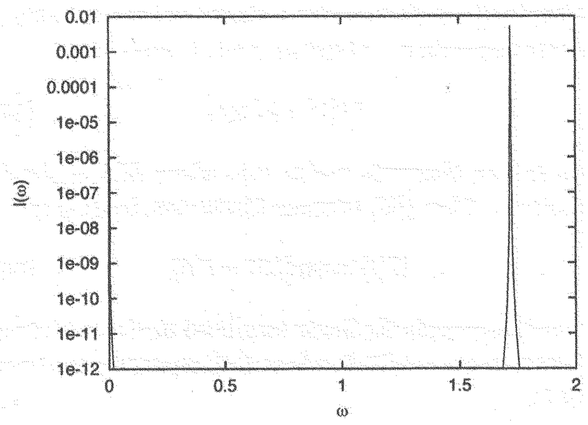


Fig. 3 Power spectrum of X is shown at $R = 1.8346$

### 3.2.2 Period-Doubling at $R \simeq 1.869$

Near this value, the period-doubling bifurcation occurs. Figure.5 shows the trajectories of the phase space for the cases (a) $R = 1.869$, (b) $R = 1.8691$, and (c) $R = 1.8721$, respectively. At $R = 1.869$, the limit cycle solution occurs, and the first period doubling occurs at $R = 1.8691$, and at $R = 1.8721$ the second period doubling occurs. The successive period-doubling occurs as $R$ increases. Associated time evolution of $X$ for each case is shown in Figure.5. In order to show the period doubling process the power spectrum for each case is shown in Figure.7. After the successive period-doubling transitions, the system becomes chaotic.

### 3.2.3 Chaos at $R = 1.873$

At $R = 1.873$, the chaotic attractor appears. Figure.8(a) shows the trajectory of the solutions in the $X$-$Y$ phase space. This trajectory indicates the existence of chaotic attractor. Temporal evolution of $X$ is shown

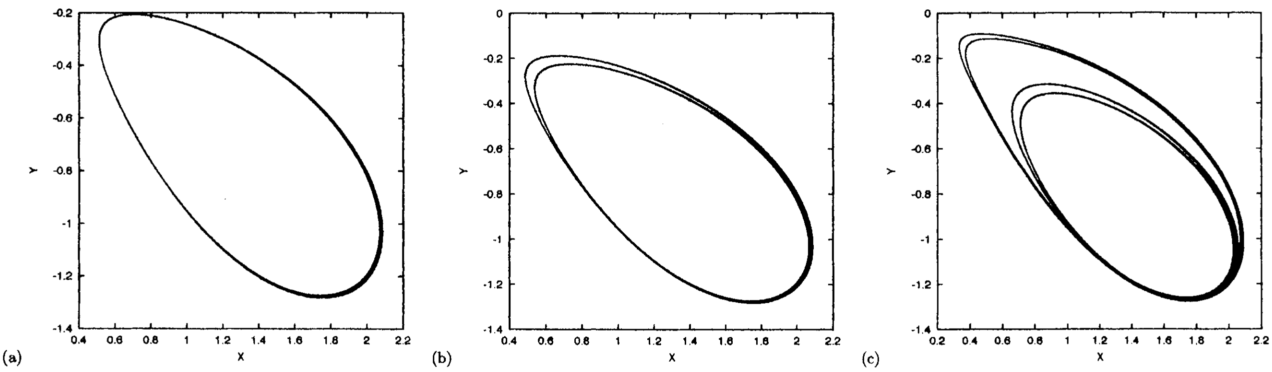


Fig. 5 Trajectory in the phase space in projected to $X$-$Y$ plane at (a) $R = 1.869$, (b) $R = 1.8691$, and (c) $R = 1.8721$.

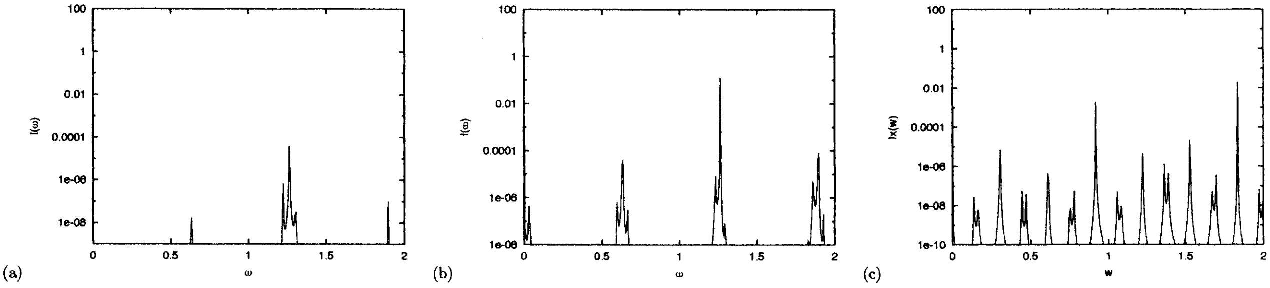


Fig. 6 Power spectrum of X is shown at (a) $R = 1.869$, (b) $R = 1.8691$, and (c) $R = 1.8721$

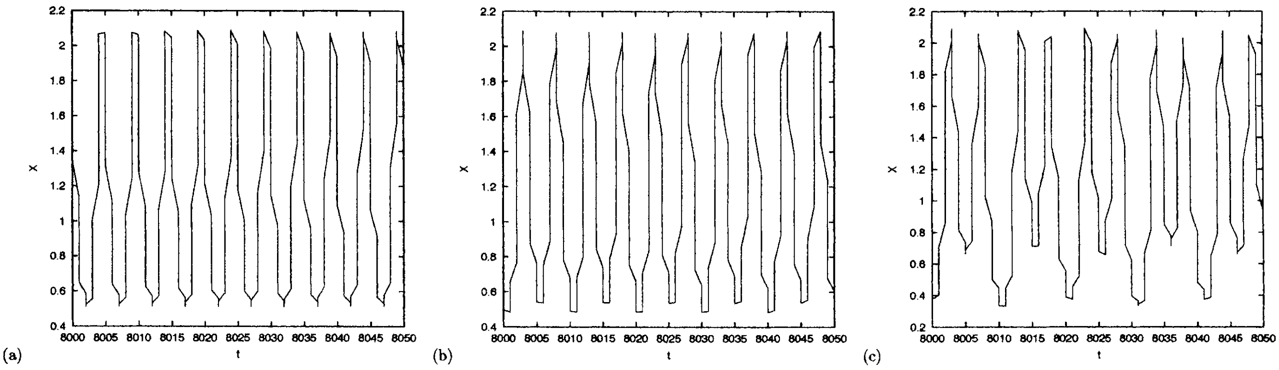


Fig. 7 Time evolution of X is shown at (a) $R = 1.869$, (b) $R = 1.8691$, and (c) $R = 1.8721$

in Figure.8(b), indicating the irregular oscillation. The chaotic attractor the projection of different phase space are shown in Figure.9.

### 3.3 Time correlation function $C_X(t)$ and power spectrum $I_X(\omega)$

The time correlation function $C_X(t)$ is defined by

$$C_X(t) \equiv \langle X(t)X(0)\rangle = \lim_{T\to\infty} \frac{1}{T}\int_0^T ds\ X(t+\tau)X(\tau), \tag{64}$$

which is used to analyze the statistical properties of chaotic orbits. In numerical simulation, we replace the time integral by the sum over data with the discreate time series $t_i = i\Delta t (i = 0, 1, 2, \ldots)$,

$$C_X(t) = \frac{1}{N}\sum_{i=0}^{N-1} X(t + i\Delta t)X(i\Delta t), \tag{65}$$

where we take a small time interval $\Delta t = T/2^6 = 2\pi/64$ with $N = 10^7$.

Figure.10 shows the result from DNS of time correlation function $C_X(t)$ with $R = 1.873$ (chaotic case). The time correlation function is related with the Fourier transform of the power spectrum of $X(t)$ according to the Wiener-Khintchine formula.

It indicates a systematic large-scale motion of $X(t)$ with a correlation time $\tau_M \simeq 50$. The time series $X(t)$ shown in Figure.8(b) consists of successive random oscil-

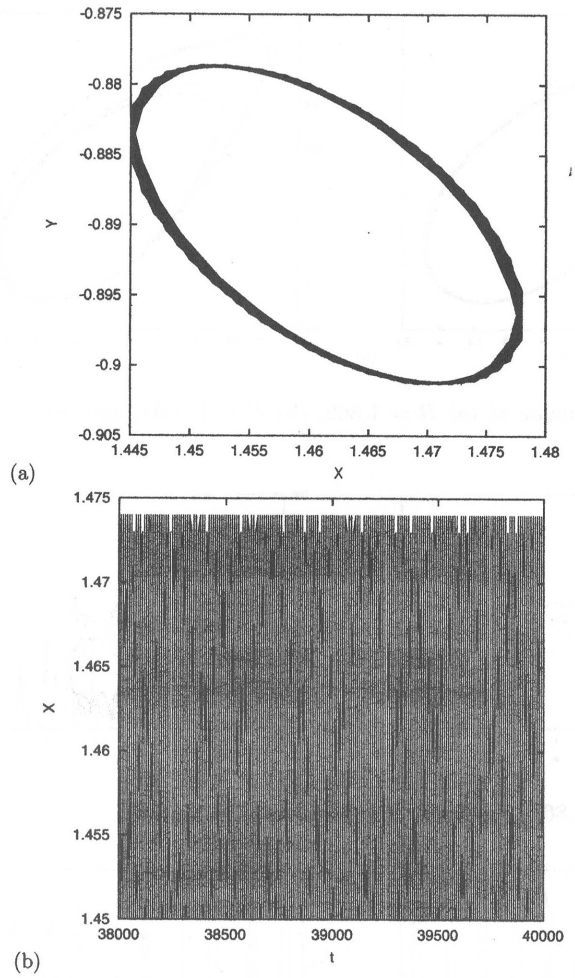


Fig. 4 (a)Trajectory in the phase space in projected to $X$-$Y$ plane at $R = 1.8346$. (b)Time evolution of $X$ is shown at $R = 1.8346$

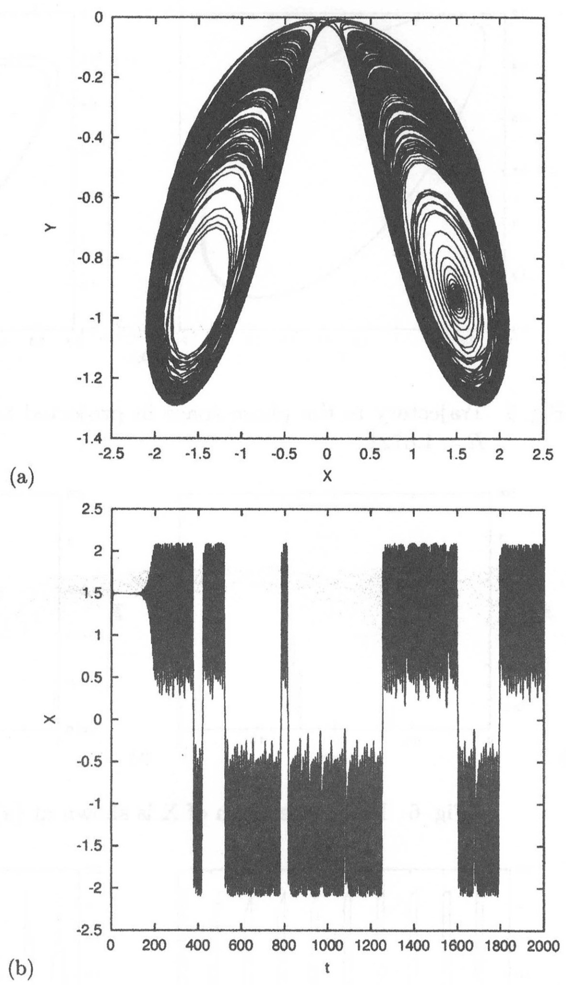


Fig. 8 (a)Trajectory in the phase space in projected to $X$-$Y$ plane at $R = 1.873$. (b)Time evolution of $X$ is shown at $R = 1.873$

lations with period $T = 2\pi$ due to a random fluctuating force which is specified by a random small-scale motion with a correlation time $\tau_r(< \tau_M)$

The power spectrum of $X(t)$ is defined by

$$
\begin{aligned}
I_X(\omega) &\equiv \lim_{\tau\to\infty} \frac{\tau}{2\pi}\left\langle\left|\frac{1}{\tau}\int_0^\tau dt\; X(t)e^{-i\omega t}\right|^2\right\rangle, \\
&= \lim_{\tau\to\infty} \frac{1}{\pi}\int_0^\tau dt \left(1-\frac{t}{\tau}\right) C_X(t)\cos(\omega t).
\end{aligned}
\tag{66}
$$

The power spectrum $I_X(\omega)$ gives an important information on the structure of the systematic large-scale motion of $X(t)$ indicated by the time correlation function $C_X(t)$. In computing Eq.(66), we replace the time integral by the sum over data with the discreate time series $t_m = m\Delta t (m = 0, 1, 2, \dots)$ and set $\tau = N'\Delta t$:

$$
I_X(\omega) = \frac{\tau}{2\pi}\frac{1}{N}\sum_{l=0}^{N-1}\left|\frac{1}{N'}\sum_{m=0}^{N'-1} X(l\Delta t + m\Delta t)e^{-i\omega m\Delta t}\right|^2,
\tag{67}
$$

where $\Delta t = T/2^6 = 2\pi/64$ and $N' = 2^{12} = 4096$.

Figure.11 shows the power spectrum $I_X(\omega)$ in the case with $R = 1.873$. It is seen four sharp peaks exist at frequencies $\omega = 0,\ \omega_1,\ \omega_2,\ \omega_1 + \omega_2$, where $\omega_1 = 1.22$, $\omega_2 = 0.605$, $\omega = 2\pi f$. These peaks are produced by the chaotic orbits. In the vicicity of $\omega = 0$, the power spectrum $I_X(\omega)$ could be approximated by Lorentian spectrum

$$
I_X(\omega) = \frac{A}{\pi}\frac{\gamma}{\omega^2 + \gamma^2},
\tag{68}
$$

which is shown in Figure.12, where $A \simeq 1.00374$, $\gamma \simeq 0.01622$, $I_X(0) = A/\pi\gamma \simeq 19.708$. According to the Wiener-Khintchine formula, this is equivalent to the

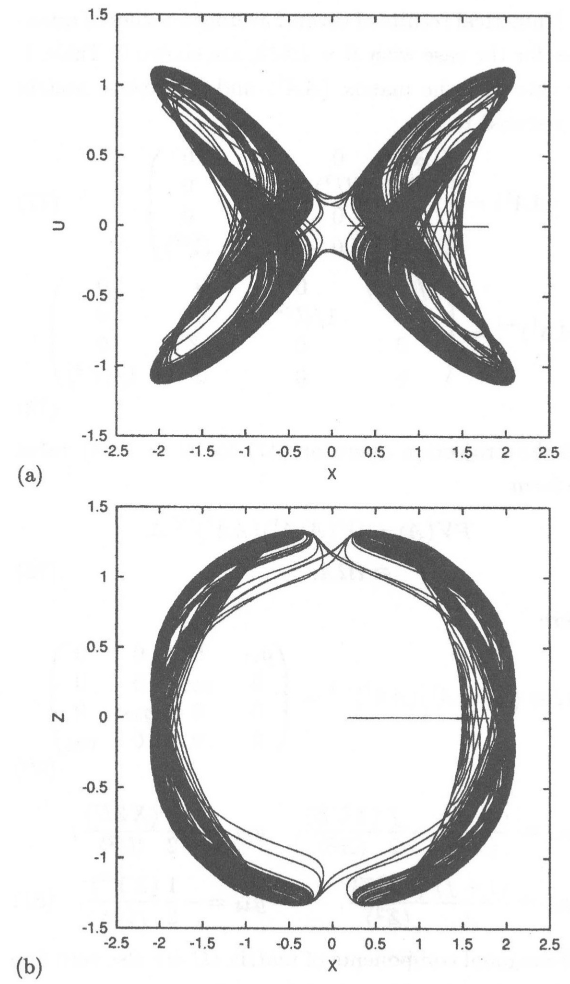


Fig. 9 (a)Trajectory in the phase space in projected to $X$-$U$ plane at $R = 1.873$. (b)Trajectory in the phase space in projected to $X$-$Z$ plane at $R = 1.873$.

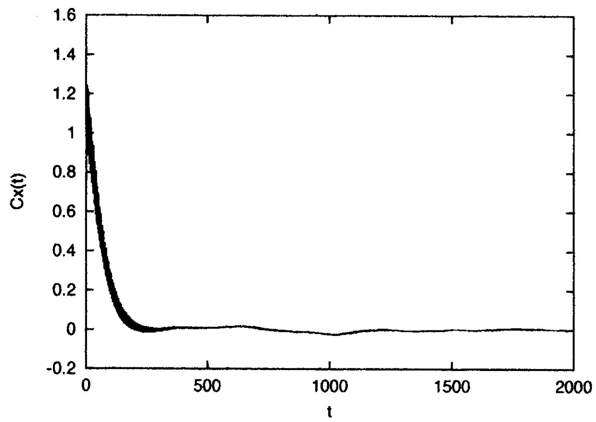


Fig. 10 The DNS of $C_X(t)$ for $R = 1.873$ obtained from Eq.(65) with $\Delta t = 2\pi/64$ and $N = 10^7$.

time correlation function

$$C_X(t) = A\exp[-\gamma t]. \tag{69}$$

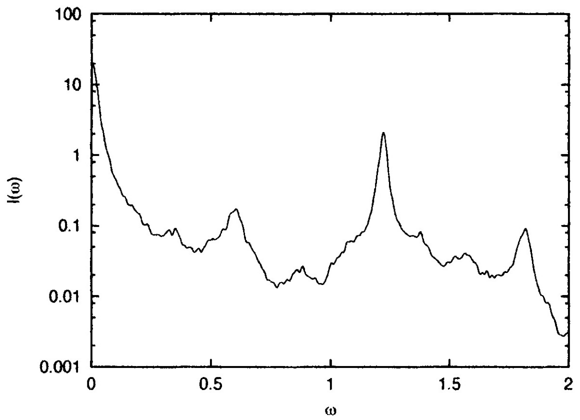


Fig. 11 Power spectrum (67) for $R = 1.873$ with $\Delta t = 2\pi/64, N' = 2^{12}$ and $N = 10^7$.

The other three peaks may also be approximated by the Lorentzian spectra.

Then, the four sharp peaks of $I_X(\omega)$ lead to the $C_X(t)$ consists of four terms:

$$\begin{aligned} C_X(t) = & \ 1.00374\exp[-0.01622t] \\ & + 0.19049\exp[-0.0144t]\cos(1.2206t + 0.0188) \\ & + 0.06097\exp[-0.0583t]\cos(0.6053t - 0.6562) \\ & + 0.01913\exp[-0.0333t]\cos(1.8199t - 0.4064). \end{aligned} \tag{70}$$

Figure.12 shows comparison between the results of DNS and Eq.(70), where $C_X(0) = 1.274$. We obtain $\tau_M \simeq 10T$, $(T = 2\pi)$ for the correlation time $\tau_M$ of the systematic large-scale motion of $X(t)$ which is consistent with the value evaluated by numerical simulation.

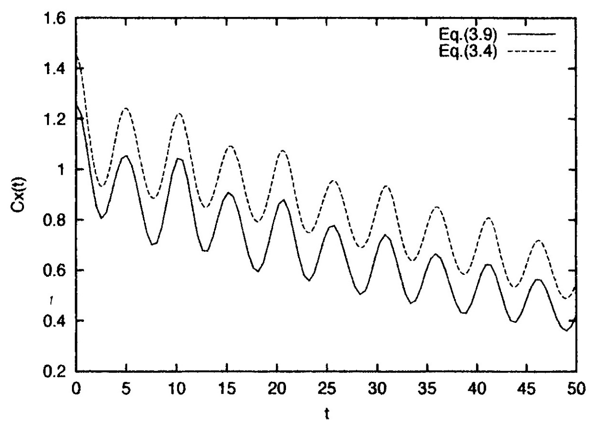


Fig. 12 $C_X(t)$ of Eq.(70) compared with that of Fig.10

# 4. Stochastic evolution equations for the VZSC model

## 4.1 Non-Markovian linear stochastic equation

We explore the fluctuations of the macrovariables $A(t) = \{X(t), U(t), Z(t), \hat{Y}(t) = Y(t) - \langle Y \rangle\}$ given by Eq.(13). It is schematically written by

$$\frac{dA(t)}{dt} = \dot{A}(t) = \Lambda A(t), \tag{71}$$

where the Liouville operator $\Lambda$ is introduced by

$$\Lambda \equiv \sum_{j=1}^{4} \dot{X}_j \frac{\partial}{\partial X_j} = \dot{X}\frac{\partial}{\partial X} + \dot{U}\frac{\partial}{\partial U} + \dot{Z}\frac{\partial}{\partial Z} + \dot{\hat{Y}}\frac{\partial}{\partial \hat{Y}}. \tag{72}$$

Then we have the schematic solution as $A(t) = \exp(t\Lambda)A$. where $X_j = X_j(t=0), A = A(t=0), X_1 = X, X_2 = U, X_3 = Z, X_4 = \hat{Y}$. As we see later, the long term averages of $X(t), U(t)$ and $Z(t)$ are zero from the symmetry property of VZSC model, while that of $Y(t)(\langle Y \rangle \equiv \lim_{\tau\to\infty} \frac{1}{\tau}\int_0^\tau dtY(t))$ is finite. Therefore we introduce the valuable $\hat{Y}(t) = Y(t) - \langle Y \rangle$ in $A(t)$ instead of $Y(t)$ .

The evolution equations of macrovariables $A(t)$ are devided into three terms:

$$\dot{A}(t) = K + LA(t) + V(A(t)), \tag{73}$$

where $K$ is constant term, $LA(t)$ is linear term, and $V(A(t))$ is nonlinear term.

For Eq.(13), these terms are explicitly written as

$$K = \begin{pmatrix} 0 \\ 0 \\ 0 \\ -e\langle Y \rangle \end{pmatrix}, V(A(t)) = \begin{pmatrix} X\hat{Y} - fUZ/2 \\ -XZ/2 \\ (1+f)UX/4 \\ -X^2/2 \end{pmatrix},$$
$$L = \begin{pmatrix} \nu(R-1) + \langle Y \rangle & 0 & 0 & 0 \\ 0 & \nu f(R-f) & 0 & 0 \\ 0 & 0 & -e/16 & 0 \\ 0 & 0 & 0 & -e \end{pmatrix}. \tag{74}$$

In Eq.(13), there are two invariances under the transformation:

(a) $X \to -X, Z \to -Z$

(b) $X \to -X, U \to -U$

Using these invariances the following relations are obtained as

$$\langle X \rangle = \langle U \rangle = \langle Z \rangle = 0,$$
$$\langle XZ \rangle = \langle X\hat{Y} \rangle = \langle UZ \rangle = \langle U\hat{Y} \rangle = \langle XU \rangle = \langle Z\hat{Y} \rangle = 0. \tag{75}$$

Since $\langle \dot{A}(t) \rangle = 0$, we have the relation $\langle V(A(t)) \rangle = -K$, which gives

$$\langle Y \rangle = -\frac{\langle X^2 \rangle}{2e}. \tag{76}$$

Numerical results of several averaged values of quantities for the case with $R = 1.873$, are shown in Table 1. For this case the matrix $\langle AA^\dagger \rangle$ and its inverse matrix are reduced to

$$\langle AA^\dagger \rangle = \begin{pmatrix} \langle X^2 \rangle & 0 & 0 & 0 \\ 0 & \langle U^2 \rangle & 0 & 0 \\ 0 & 0 & \langle Z^2 \rangle & 0 \\ 0 & 0 & 0 & \langle \hat{Y}^2 \rangle \end{pmatrix}, \tag{77}$$

$$\langle AA^\dagger \rangle^{-1} = \begin{pmatrix} 1/\langle X^2 \rangle & 0 & 0 & 0 \\ 0 & 1/\langle U^2 \rangle & 0 & 0 \\ 0 & 0 & 1/\langle Z^2 \rangle & 0 \\ 0 & 0 & 0 & 1/\langle \hat{Y}^2 \rangle \end{pmatrix}, \tag{78}$$

and the projection operator (47) for $G = V(A)$ takes the form

$$\mathcal{P}V(A) = \langle V(A)A^\dagger \rangle \langle AA^\dagger \rangle^{-1} A,$$
$$\equiv i\Omega A, \tag{79}$$

where

$$i\Omega \equiv \langle V(A)A^\dagger \rangle \langle AA^\dagger \rangle^{-1} = \begin{pmatrix} g_{11} & 0 & 0 & 0 \\ 0 & g_{22} & 0 & 0 \\ 0 & 0 & g_{33} & 0 \\ 0 & 0 & 0 & g_{44} \end{pmatrix}, \tag{80}$$

$$g_{11} = \frac{\langle X^2\hat{Y} \rangle}{\langle X^2 \rangle} - \frac{f}{2}\frac{\langle XUZ \rangle}{\langle X^2 \rangle}, \quad g_{22} = -\frac{1}{2}\frac{\langle XZU \rangle}{\langle U^2 \rangle},$$
$$g_{33} = \frac{(1+f)}{2}\frac{\langle UXZ \rangle}{\langle Z^2 \rangle}, \quad g_{44} = -\frac{1}{2}\frac{\langle X\hat{Y}^2 \rangle}{\langle \hat{Y}^2 \rangle}. \tag{81}$$

Off-diagonal components of matrix $i\Omega$ are also zero due to the symmetry property (a) and (b) as:

$$\langle X\hat{Y}U \rangle = \langle UZ^2 \rangle = \langle X\hat{Y}^2 \rangle = \langle UZ\hat{Y} \rangle = 0,$$
$$\langle XZ\hat{Y} \rangle = \langle U^2X \rangle = \langle X^3 \rangle = \langle X^2U \rangle = 0,$$
$$\langle X\hat{Y}U \rangle = \langle U^2Z \rangle = \langle X^2Z \rangle = \langle XZ^2 \rangle = \langle UX\hat{Y} \rangle = 0. \tag{82}$$

Numerical results of the components of matrix $i\Omega$ for the case with $R = 1.873$, are tabled in Table 2. The diagonal components are dominant contributions in the numerical simulations except for the value of $g_{32}$. As is shown in the reference[9], Eq.(73) can be transformed into a non-Markovian linear stochastic equation in the following manner:

$$\dot{A}(t) = K + LA(t) + V(A(t)), \tag{83}$$
$$== K + LA(t) + e^{t\Lambda}V(A), \tag{84}$$
$$= K + LA(t) + e^{t\Lambda}\{\mathcal{P} + \mathcal{Q}\}V(A), \quad (\because \mathcal{Q} \equiv 1 - \mathcal{P}), \tag{85}$$
$$= K + (L + i\Omega)A(t) + e^{t\Lambda}\mathcal{Q}V(A), \tag{86}$$
$$= K + (L + i\Omega)A(t) + e^{t\mathcal{Q}\Lambda}\mathcal{Q}V(A) \tag{87}$$
$$+ \int_0^t ds\ e^{(t-s)\Lambda}\mathcal{P}\Lambda e^{s\mathcal{Q}\Lambda}\mathcal{Q}V(A), \tag{88}$$
$$= K + (L + i\Omega)A(t) + R(t) - \int_0^t ds\ \Gamma(s)A(t-s). \tag{89}$$

Table 1 Long-time average of several quantities for $R = 1.873$ with $N = 10^7$

| $\langle X \rangle$ | $\langle U \rangle$ | $\langle Z \rangle$ | $\langle Y \rangle$ | $\langle XU \rangle$ | $\langle XZ \rangle$ | $\langle X\hat{Y} \rangle$ |
|---|---|---|---|---|---|---|
| $-1.92 \times 10^{-2}$ | $-0.93 \times 10^{-4}$ | $-5.70 \times 10^{-3}$ | -0.604 | $-8.42 \times 10^{-4}$ | $1.66 \times 10^{-4}$ | $3.15 \times 10^{-3}$ |
| $\langle UZ \rangle$ | $\langle U\hat{Y} \rangle$ | $\langle Z\hat{Y} \rangle$ | $\langle X^2 \rangle$ | $\langle U^2 \rangle$ | $\langle Z^2 \rangle$ | $\langle \hat{Y}^2 \rangle$ |
| $-3.15 \times 10^{-3}$ | $-2.73 \times 10^{-5}$ | $-3.62 \times 10^{-3}$ | 1.45 | 0.414 | 1.15 | 0.152 |

Table 2 Numerical analysis of matrix $i\Omega$ for $R = 1.873$ with $N = 10^7$

| $g_{11}$ | $g_{12}$ | $g_{13}$ | $g_{14}$ |
|---|---|---|---|
| $-3.28 \times 10^{-1}$ | $3.08 \times 10^{-3}$ | $-4.38 \times 10^{-4}$ | $-2.63 \times 10^{-2}$ |
| $g_{21}$ | $g_{22}$ | $g_{23}$ | $g_{24}$ |
| $-5.03 \times 10^{-4}$ | $-1.49 \times 10^{-1}$ | $6.68 \times 10^{-3}$ | $5.55 \times 10^{-3}$ |
| $g_{31}$ | $g_{32}$ | $g_{33}$ | $g_{34}$ |
| $2.98 \times 10^{-4}$ | $-1.82 \times 10^{-2}$ | $7.49 \times 10^{-2}$ | $1.97 \times 10^{-3}$ |
| $g_{41}$ | $g_{42}$ | $g_{43}$ | $g_{44}$ |
| $1.43 \times 10^{-2}$ | $-7.48 \times 10^{-4}$ | $-6.63 \times 10^{-4}$ | 1.20 |

with the aid of the operator identity Eq.(47), where we introduce the fluctuating force $R(t)$ and the memory function $\Gamma(t)$ given by

$$R(t) \equiv e^{tQ\Lambda}QV(A) = \begin{pmatrix} r_X(t) \\ r_U(t) \\ r_Z(t) \\ r_Y(t) \end{pmatrix} = \begin{pmatrix} e^{tQ\Lambda}Q(X\hat{Y} - fUZ/2) \\ -e^{tQ\Lambda}Q(XZ/2) \\ (1+f)e^{tQ\Lambda}Q(UX/4) \\ -e^{tQ\Lambda}Q(X^2/2) \end{pmatrix}, \tag{90}$$

$$\Gamma(t) \equiv \langle R(t)R(0)\rangle\langle AA^\dagger\rangle^{-1} = \begin{pmatrix} \gamma_{11}(t) & 0 & 0 & 0 \\ 0 & \gamma_{22}(t) & 0 & 0 \\ 0 & 0 & \gamma_{33}(t) & 0 \\ 0 & 0 & 0 & \gamma_{44}(t) \end{pmatrix}, \tag{91}$$

where

$$\gamma_{11}(t) = \frac{\langle r_X(t)r_X(0)\rangle}{\langle X^2\rangle}, \gamma_{22}(t) = \frac{\langle r_U(t)r_U(0)\rangle}{\langle U^2\rangle},$$
$$\gamma_{33}(t) = \frac{\langle r_Z(t)r_Z(0)\rangle}{\langle Z^2\rangle}, \gamma_{44}(t) = \frac{\langle r_Y(t)r_Y(0)\rangle}{\langle \hat{Y}^2\rangle}. \tag{92}$$

Off-diagonal components of matrix $\Gamma(t)$ are also zero due to the symmetry property:
$\Lambda \to -\Lambda$, $\mathcal{P} \to \mathcal{P}$, $\mathcal{Q} \to \mathcal{Q}$, then $r_X \to -r_X$, $r_U \to -r_U$, $r_Z \to r_Z$, $r_Y \to r_Y$, which implies

$$\langle r_X r_Y\rangle = \langle r_Y r_X\rangle = 0. \tag{93}$$

Therefore, each component of the evolution equation is given by

$$\dot{X}(t) = \{\nu(R-1) + \langle Y\rangle + g_{11}\}X(t) + r_X(t) - \int_0^t ds\ \gamma_{11}(s)X(t-s), \tag{94}$$

$$\dot{U}(t) = \{\nu f(R-f) + g_{22}\}U(t) + r_U(t) - \int_0^t ds\ \gamma_{22}(s)U(t-s), \tag{95}$$

$$\dot{Z}(t) = \left(-\frac{e}{16} + g_{33}\right) Z(t) + r_Z(t) - \int_0^t ds\ \gamma_{33}(s)Z(t-s), \tag{96}$$

$$\dot{\hat{Y}}(t) = -e\langle Y\rangle(-e + g_{44})\hat{Y}(t) + r_Y(t) - \int_0^t ds\ \gamma_{44}(s)\hat{Y}(t-s). \tag{97}$$

The time-evolution of $R(t)$ and $\Gamma(t)$ is governed by the modified propagator $e^{tQ\Lambda}$. The Laplace transform $\Gamma(z)$ of Eq.(91) gives the frequency-dependent transport coefficient $\Gamma(i\omega)$ induced by chaos.

The integrand of the third term of Eq.(87) has the factor

$$\mathcal{P}\Lambda e^{sQ\Lambda}QV(A) = \mathcal{P}\Lambda R(s) = \langle\{\Lambda R(s)\}A^\dagger\rangle\langle AA^\dagger\rangle^{-1}. \tag{98}$$

Since $\langle\{\Lambda R(s)\}A^\dagger\rangle = -\langle R(t)(\Lambda A)^\dagger\rangle = -\langle R(t)(Q\Lambda A)^\dagger\rangle = -\langle R(t)R^\dagger\rangle$, this gives

$$\mathcal{P}R(t) = -\langle R(t)R^\dagger\rangle\langle AA^\dagger\rangle^{-1}. \tag{99}$$

Then, the third term of Eq.(87) reduces the third term of Eq.(89). In this way Eq.(73) is transformed into the non-Markovian linear stochastic equation Eq.(89).

The time series $X(t)$ in Figure.8(b) is dictated by Eq.(73) that is equivalent to Eq.(13), so that its successive random fluctuations are created by the fluctuating force $R(t)$. Since $\langle R(t)X(0)\rangle = 0$, $C(t) \equiv \langle A(t)A(0)\rangle$, then we obtain the evolution equation for the time correlation:

$$\dot{C}(t) = (L + i\Omega)C(t) - \int_0^t ds\ \Gamma(s)C(t-s). \quad (100)$$

This is a linear equation for $C(t)$ and can be integrated to give an explicit expression for $C(t)$. It indicates that the time correlation function $C(t)$ gives the average regression of fluctuations of $A(t)$ from a given chaotic state. Thus it turns out that the necessary effects due to the nonlinear force $V(A)$ are all included in the memory function $\Gamma(s)$, which implies the closure problem does not occur in this Mori's projection operator method.

### 4.2 Memory function $\Gamma(t)$ and force correlation $\Phi(t)$

In this section, we integrate a non-Markovian evolution equation for $C(t)$ and explore the $\omega$ dependence of the transport coefficient $\Gamma(i\omega)$.

### 4.3 Time correlation function $C(t)$ in terms of the force correlation $\Phi(t)$

It is difficult to compute the time evolution of the fluctuating force (90) directly. Therefore, using Eq.(86) and (89), let us consider the nonlinear force

$$F(t) \equiv e^{tA}QV(A) = R(t) - \int_0^t ds\ \Gamma(s)A(t-s),$$
$$= \begin{pmatrix} f_X(t) \\ f_U(t) \\ f_Z(t) \\ f_Y(t) \end{pmatrix} = \begin{pmatrix} X\hat{Y} - fUZ/2 - g_{11}X \\ -XZ/2 - g_{22}U \\ (1+f)UX/4 - g_{33}Z \\ -X^2/2 - g_{44}\hat{Y} \end{pmatrix}, \quad (101)$$

then, we have

$$\dot{A}(t) = K + (L + i\Omega)A(t) + F(t). \quad (102)$$

The time correlation of $F(t)$ is defined by

$$\Phi(t) \equiv \langle F(t)F(0)\rangle\langle AA^\dagger\rangle^{-1}$$
$$= \begin{pmatrix} \phi_{11}(t) & 0 & 0 & 0 \\ 0 & \phi_{22}(t) & 0 & 0 \\ 0 & 0 & \phi_{33}(t) & 0 \\ 0 & 0 & 0 & \phi_{44}(t) \end{pmatrix}, \quad (103)$$

where

$$\phi_{11}(t) = \frac{\langle f_X(t)f_X(0)\rangle}{\langle X^2\rangle}, \phi_{22}(t) = \frac{\langle f_U(t)f_U(0)\rangle}{\langle U^2\rangle},$$
$$\phi_{33}(t) = \frac{\langle f_Z(t)f_Z(0)\rangle}{\langle Z^2\rangle}, \phi_{44}(t) = \frac{\langle f_Y(t)f_Y(0)\rangle}{\langle \hat{Y}^2\rangle}. \quad (104)$$

Off-diagonal components of matrix $\Phi(t)$, are zero due to the symmetry property

(a): $f_X \to -f_X,\ f_U \to -f_U,\ f_Z \to f_Z,\ f_Y \to f_Y,$

$$\therefore \langle f_X f_Z\rangle = \langle f_X f_Y\rangle = \langle f_U f_Z\rangle = \langle f_U f_Y\rangle = 0. \quad (105)$$

(b): $f_X \to -f_X,\ f_U \to f_U,\ f_Z \to -f_Z,\ f_Y \to f_Y,$

$$\therefore \langle f_X f_U\rangle = \langle f_Z f_Y\rangle = 0. \quad (106)$$

Figure.13 shows the result from DNS of $\phi_{11}(t)$ for $R = 1.873$.

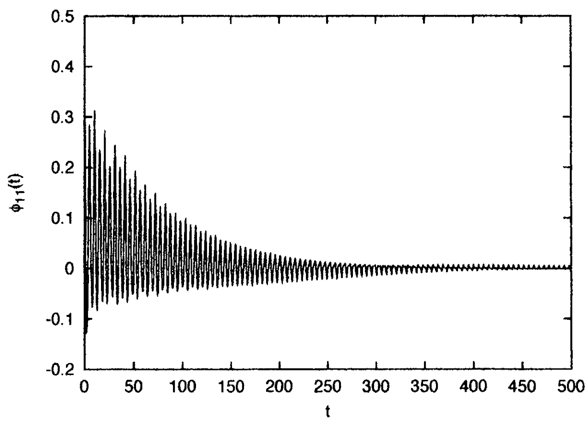


Fig. 13 The DNS of $\phi_{11}(t)$ for $R = 1.873$ with $\Delta t = 2\pi/64$ and $N = 10^7$.

Inserting Eq.(101) into Eq.(103) leads to

$$\Phi(t) = \Gamma(t) - \int_0^t ds\ \Gamma(t-s)\langle A(s)R^\dagger(0)\rangle\langle AA^\dagger\rangle^{-1}. \quad (107)$$

Taking the Laplace transform of Eq.(107), we obtain

$$\Phi(z) \equiv \int_0^\infty dt\, e^{-zt}\Phi(t) = \Gamma(z) - \Gamma(z)\langle A(z)R^\dagger\rangle\langle AA^\dagger\rangle^{-1}. \quad (108)$$

On the other hand, the Laplace transform of Eq.(102) leads to

$$A(z) = \Upsilon(z)\{F(z) + A(0)\}, \quad (109)$$

where

$$\Upsilon(z) = \begin{pmatrix} 1/c_{11} & 0 & 0 & 0 \\ 0 & 1/c_{22} & 0 & 0 \\ 0 & 0 & 1/c_{33} & 0 \\ 0 & 0 & 0 & 1/c_{44} \end{pmatrix}, \quad (110)$$

$$c_{11} = z - \{\nu(R-1) + \langle Y\rangle\} - g_{11}, \quad c_{22} = z - \nu f(R-f) - g_{22}$$
$$c_{33} = z + e/16 - g_{33}, \quad c_{44} = z + e - g_{44}. \quad (111)$$

Substituting Eq.(109) into Eq.(108), we have

$$\Phi(z) = \Gamma(z) - \Gamma(z)\Upsilon(z)\Phi(z). \quad (112)$$

This gives the relation between the force correlation and memory function. That is we can calculate $\Gamma(t)$ via $F(t) \to \Phi(t) \to \Gamma(t)$.

We now integrate the evolution equation Eq.(100) for

$C(t)$, and derive an explicit form of $C(t)$ in terms of $\Phi(t)$. Taking the Laplace transform of Eq.(100) leads to

$$zC_{ii}(z)-\langle A_i^2\rangle = \lambda_i C_{ii}(z)-\gamma_{ii}(z)C_{ii}(z), \quad (i=X,U,Z,Y). \tag{113}$$

$$\therefore C_{ii}(z) = \frac{\langle A_i^2\rangle}{z-\lambda_i+\gamma_{ii}(z)}, \tag{114}$$

where $\lambda_i \equiv L_{ii}+g_{ii}, A_1 = X, A_2 = U, A_3 = Z, A_4 = \hat{Y}$. In order to simplify the equation, we use the component of matrix. Using Eq.(112), we get the equation

$$C_{ii}(z) = \langle A_i^2\rangle \left\{\frac{1}{z-\lambda_i} - \frac{\phi_{ii}(z)}{(z-\lambda_i)^2}\right\}. \tag{115}$$

The inversion of the Laplace transform of Eq.(115) leads to

$$C_{ii}(t) = \langle A_i^2\rangle \left\{e^{\lambda_i t} - e^{\lambda_i t}\int_0^t ds\, e^{-\lambda_i s}(t-s)\phi_{ii}(s)\right\}. \tag{116}$$

This equation shows the time correlation function $C(t)$ explicitly in terms of $\Phi(t)$.

### 4.4 $\omega$-dependent transport coefficients $\gamma_{jj}(i\omega)$ in terms of $\phi_{jj}(i\omega)$

We write $\gamma_{ii}(z)$ and $\phi_{ii}(z)$ as follows:

$$\gamma_{jj}(i\omega) \equiv \int_0^t dt\, e^{-i\omega t}\gamma_{jj}(t) = \gamma'_{jj}(\omega)+i\gamma''_{jj}(\omega), \tag{117}$$

$$\phi_{jj}(i\omega) \equiv \int_0^t dt\, e^{-i\omega t}\phi_{jj}(t) = \phi'_{jj}(\omega)+i\phi''_{jj}(\omega), \tag{118}$$

where $z = i\omega$, the prime indicates the real part and double prime, the imaginary part respectively. Substituting Eq.(117) into Eq.(115) we calculate

$$C_{jj}(i\omega) = \frac{\langle A_j^2\rangle}{i\{\omega+\gamma''_{jj}(\omega)\}+\gamma'_{jj}(\omega)-\lambda_j}, \tag{119}$$

$$= \frac{\langle A_j^2\rangle[\{\gamma'_{jj}(\omega)-\lambda_j\}-i\{\omega+\gamma''_{jj}(\omega)\}]}{\{\omega+\gamma''_{jj}(\omega)\}^2+\{\gamma'_{jj}(\omega)-\lambda_j\}^2}. \tag{120}$$

The power spectrum is given by

$$I_{A_i}(\omega) = \frac{\langle A_i^2\rangle}{\pi}\frac{\{\gamma'_{ii}(\omega)-\lambda_i\}}{\{\omega+\gamma''_{jj}(\omega)\}^2+\{\gamma'_{jj}(\omega)-\lambda_j\}^2}. \tag{121}$$

The term $\gamma_{jj}(i\omega)$ is the $\omega$-dependent chaotic transport coefficient which gives the frequency $\omega_j$ and the damping $\widetilde{\gamma}_j$ for the average regressions of chaotic fluctuations. The relation $\omega_i = -\gamma''_{ii}(\omega_i)$ introduces a real frequency $\omega_i$. Neglecting the $\omega$ dependence of $\gamma'_{ii}(\omega)$ around $\omega=\omega_i$, then it reduces Lorentzian spectra

$$I_{A_i}(\omega) \simeq \frac{\langle A_i^2\rangle}{\pi}\frac{\widetilde{\gamma}_i}{\{\omega-\omega_i\}^2+\widetilde{\gamma}_i{}^2}, \tag{122}$$

where $\widetilde{\gamma}_i \equiv \gamma'_{ii}(\omega_i)-\lambda_i$. Using Wiener-Khinchine formula, we obtain

$$C_{ii}(t) \simeq \sum_i a_{ij}e^{-\widetilde{\gamma_{ij}}t}\cos(\omega_{ij}t+\varphi_{ij}). \tag{123}$$

Since $\langle A_j(0)r_j(0)\rangle = \langle r_j(0)\rangle = 0$ for $j\neq 4$, Eq.(112) gives

$$\phi_{jj}(z) = \gamma_{jj}(z)-\gamma_{jj}(z)\frac{\langle A_j(z)r_j(0)\rangle}{\langle A_j^2\rangle},$$

$$= \gamma_{jj}(z)-\gamma_{jj}(z)\frac{1}{z-\lambda_j}\phi_{jj}(z). \tag{124}$$

$$\therefore \frac{1}{\gamma_{jj}(z)} = \frac{1}{\phi_{jj}(z)} - \frac{1}{z-\lambda_i}. \tag{125}$$

for $j\neq 4$, we calculate

$$\gamma_{jj}(i\omega) = \frac{\{i\omega-\lambda_j\}\phi_{jj}(i\omega)}{i\omega-\lambda_j-\phi'_{jj}(i\omega)},$$

$$= \frac{i\{\omega\phi'_{jj}(\omega)-\lambda_j\phi''_{jj}(\omega)\}-\{\omega\phi''_{jj}(\omega)+\lambda_j\phi'_{jj}(\omega)\}}{i\{\omega-\phi''_{jj}(\omega)\}-\{\lambda_j+\phi'_{jj}(\omega)\}}. \tag{126}$$

The real part and the imaginary part of $\gamma_{jj}(i\omega)$ are explicitely written as

$$\gamma'_{jj}(\omega) = \frac{\{\omega\phi'_{jj}(\omega)-\lambda_j\phi''_{jj}(\omega)\}\alpha+\{\omega\phi''_{jj}(\omega)+\lambda_j\phi'_{jj}(\omega)\}\beta}{\alpha^2+\beta^2},$$

$$\gamma''_{jj}(\omega) = \frac{-\{\omega\phi'_{jj}(\omega)-\lambda_j\phi''_{jj}(\omega)\}\beta+\{\omega\phi''_{jj}(\omega)+\lambda_j\phi'_{jj}(\omega)\}\alpha}{\alpha^2+\beta^2}. \tag{127}$$

where $\alpha = \omega-\phi''_{jj}(\omega)$ and $\beta = \lambda_j+\phi'_{jj}(\omega)$. Since $K_4 = -e\langle Y\rangle$ for $j=4$, we obtain

$$\phi_{44}(z) = \gamma_{44}(z)-\gamma_{44}(z)\frac{1}{z-\lambda_4}\left\{\phi_{44}(z)-\frac{e\langle Y\rangle}{z}\frac{\langle r_4\rangle}{\langle\hat{Y}^2\rangle}\right\}. \tag{128}$$

Since $\lambda_4 = -e+g_{44}<0,\ e\langle Y\rangle\langle r_4\rangle = (\langle X^2\rangle)^2/4$, this gives

$$\frac{1}{\gamma_{44}(z)} = \frac{1}{\phi_{44}(z)} - \frac{1}{z-\lambda_4}\left\{1-\frac{b}{z\phi_{44}(z)}\right\}, \tag{129}$$

where $b = \langle X^2\rangle^2/4\langle\hat{Y}^2\rangle$. Explicit form of $\gamma_{44}$ is written as

$$\gamma_{44}(i\omega) = \frac{\{i\omega-\lambda_4\}\phi_{44}(i\omega)}{\{i\omega-\lambda_4\}-\phi_{44}(i\omega)+\frac{b}{i\omega}},$$

$$= \frac{-i\omega\{\omega\phi''_{44}(\omega)+\lambda_4\phi'_{44}(\omega)\}-\omega\{\omega\phi'_{44}(\omega)-\lambda_4\phi''_{44}(\omega)\}}{-i\omega\{\phi'_{44}(\omega)+\lambda_4\}-\{\omega^2-\omega\phi''_{44}(\omega)-b\}}, \tag{130}$$

$$\gamma'_{44}(\omega) = \frac{C'(\omega)}{D(\omega)}, \qquad \gamma''_{44}(\omega) = \frac{C''(\omega)}{D(\omega)}, \tag{131}$$

$$D(\omega) \equiv \omega^2\{\phi'_{44}(\omega)+\lambda_4\}^2+\{\omega^2-\omega\phi''_{44}(\omega)-b\}^2, \tag{132}$$

$$C'(\omega) \equiv \omega^2\{\phi'_{44}(\omega)+\lambda_4\}\{\omega\phi''_{44}(\omega)+\lambda_4\phi'_{44}(\omega)\} + \omega\{\omega^2-\omega\phi''_{44}(\omega)-b\}\{\omega\phi'_{44}(\omega)-\lambda_4\phi''_{44}(\omega)\}, \tag{133}$$

$$C''(\omega) \equiv \omega^2\{\phi'_{44}(\omega)+\lambda_4\}\{\omega\phi''_{44}(\omega)-\lambda_4\phi'_{44}(\omega)\} + \omega\{\omega^2-\omega\phi''_{44}(\omega)-b\}\{\omega\phi'_{44}(\omega)+\lambda_4\phi''_{44}(\omega)\}. \tag{134}$$

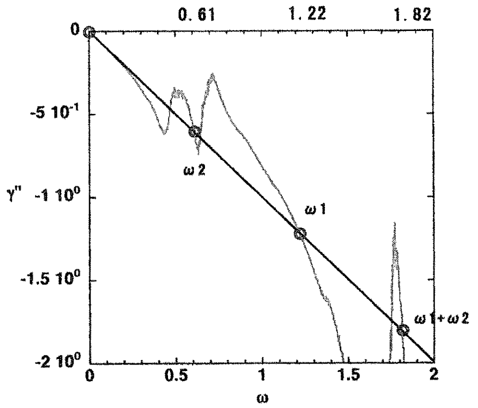


Fig. 14 $\omega$ dependent transport coefficients $\gamma''_{11}(\omega)$ obtained from (127) for $R = 1.873$.

Figure.14 shows $\gamma''_{11}(\omega)$ obtained from Eq.(127) numerically. Frequency $\omega = 0,\ 0.605(=\omega_1),\ 1.22(=\omega_2),\ 1.82(=\omega_1+\omega_2)$ correspond to four peaks of power spectrum of $X$ in Figure.11 for the relation $\omega = -\gamma''_{11}(\omega)$.

## 5. Summary and Discussion

The understanding of the basic feature of plasma turbulence is very important not only for the fusion study but also for the statistical theory. The relation between turbulence and Mori method is reported by S-I.Itoh et al[18]. In this reference, used Mori method to the model of multi degree of freedom, so in this thesis, we applied Mori method to the model with a few degrees of freedom.

The drift wave chaos is investigated using VZSC model which is the simplified model with a few degrees of freedom reduced for Hasegawa-Wakatani model. In order to simulate VZSC model given by Eq.(13), we use a fourth-order Runge-Kutta method. In this simulation, parameter $R$ is chosen as an order parameter to characterize the system behavior and the other parameters $\nu, e, f$ are fixed. It is found that for the regime $R < 1.8344$, the fixed point exists, for the regime $1.8344 \leq R \leq 1.8725$, the limit cycle appears, and for the regime $R \geq 1.872$, chaos occurs.

In order to analyze the statistical properties of chaotic orbits, we show numerical results of the time correlation function $C_X(t)$ and the power spectrum $I_X(\omega)$ at $R = 1.873$ according to the definition. It is found that a systematic large-scale motion of $X(t)$ has a correlation time $\tau_M \simeq 50$, and power spectrum of $X$ has four sharp peaks at frequencies $\omega = 0,\ 0.605(=\omega_2),\ 1.22(=\omega_1),\ 1.82(=\omega_1+\omega_2)$. Then, fitting four peaks in the power spectrum to the Lorenzian and inverse Laplace transforming of it, we obtain $C_X(t)$ approximately. It is found that oscillation frequency of $C_X(t)$ shows a fairly good agreement with DNS results.

Next, we derived the non-Markovian linear stochastic equation for the VZSC model, applying Mori's projection operator method. It is difficult to compute the time evolution of the fluctuating force $R(t)$. Therefore first, we defined the nonlinear force $F(t)$. Secondly we calculate the correlation of $F(t)$ $(=\phi_{jj}(i\omega))$ numerically. Then using Eq.(4.39), we calculate $\omega$-dependent transport coefficients $\gamma_{jj}(i\omega)$ indirectly. It is found that four peaks of power spectrum of $X$ correspond to the solution of $\omega = -\gamma''_{11}(\omega)$. We make sure that projection operator method is an useful technique.

It is necessary to simulate the following equation

$$\gamma_{11}(t) = \frac{2}{\pi}\int_0^\infty d\omega\ \gamma''_{11}(\omega)\cos(\omega t), \qquad (135)$$

and investigate the damping form. It is left for future work.

In this thesis, the Mori's projection operator method has been applied to the plasma turbulence theory and its applicability has been confirmed through the comparison with numerical calculation. However, this is the first attempt and, in order to verify its validity, the more detail study will be required and it remains to the future work.

## Acknowledgement

The author would like to thank Prof. S. -I. Itoh for her guidance, support and continuous encouragement during the course of research, and Prof. M. Yagi for important suggestions and help to the computer simulations. Special thanks to Prof. H. Mori, Dr. M. Azumi (Japan Atomic Energy Agency) for useful discussions and comments. This work is partly supported by the Grant-in-Aid for Specially-Promoted Research of MEXT(16002005), by the Grant-in-Aid for Scientific Research of JSPS(16360459) and by the collaboration programs of NIFS and of the Research Institute for Applied Mechanics of Kyushu University.

Furthermore, the author is grateful to his colleague; Mr. S. Tokunaga, Mr. T. Hayashi and all classmates in Advanced Energy Engineering Science. he enjoyed his school life with them for 2 years.

Finally, the author thanks his family for their supports.

## References

1) R.Z.Sagdeev, V.D.Shapiro, and V.I. Shevchenko, Sov.J.Plasma Phys.**4**, 306 (1978)

2) A.A.Vasil'ev, G.M.Zaslavsky, R.Z.Sagdeev, and A.A.Chernikov, Sov.J.Plasma Phys.**16**, 681 (1991)

3) S.Benkadda, P.Gabbai, G.M.Zaslavsky Phys. Plasmas **4**, 2864 (1997)

4) A.Hasegawa and M.Wakatani, Phys Rev.Lett. **50**, 682 (1983)

5) A.Hasegawa and M.Mima, Phis Rev.Lett. **39**, 205 (1977)

6) H.Mori Prog .Theor. Phys. **33**, 423 (1965)

7) H.Mori, S.Kuroki, T.Horita, R.Ishizaki, and N.Mori Prog .Theor. Phys. **111**, 635 (2004)

8) H.Mori, S.Kuroki, T.Horita Prog .Theor. Phys. **113**, 29 (2005)

9) R.Ishizaki, H.Mori, H.Tominaga, S.Kuroki, and N.Mori Prog .Theor. Phys. **109**, 169 (2003)

10) H.Tominaga, S.Kuroki, H.Mori Prog .Theor. Phys. **109**, 575 (2003)

11) H.Mori, Y.Kuramoto "*Dissipative Structures and Chaos*" Springer-Verlag Berlin, (1998)

12) J.Guckenheimer, P.Homes, "*Nonlinear Oscillations, Dynamical Systems, and Bifurcations of Vector Fields*" Springer-Verlag Berlin, (1983)

13) E.N.Lorentz J. Atmos. Sci. **20**, 130 (1963)

14) J.Frøyland, K.H.Alfsen Phys Rev.A **29**, 2928 (1984)

15) J.E.Marsden, M.McCracken " *The Hopf Bifurcation and its Applications*" Springer, New York(1976)

16) M.Feigenbaum J. Stat. Phys. **19**, 25(1978)

17) T.Aoyagi, M.Yagi, and S-I. Itoh J. Phys. Soc. Jpn **66**, 2689 (1997)

18) Sanae-I. Itoh, Kimitaka Itoh, Hazime Mori J. Phys. Soc. Jpn,Vol.**75**, No.3 034501(1-9)(2006)


# Appendix

## A1. *-Derivation of Eq.(47)-*

Let us write $e^{t\Lambda}$ as

$$e^{t\Lambda} = e^{tQ\Lambda} + e^{t\Lambda}S(t), \tag{A1}$$

where we have defined

$$S(t) \equiv 1 - e^{-t\Lambda}e^{tQ\Lambda} = \int_0^t ds\ \frac{d}{ds}\{1 - e^{-s\Lambda}e^{sQ\Lambda}\}$$
$$= \int_0^t ds\ e^{-s\Lambda}\mathcal{P}\Lambda e^{sQ\Lambda}. \tag{A2}$$

Eq.(A2) is inserted into Eq.(A1) to give (47)

$$e^{t\Lambda} = e^{tQ\Lambda} + \int_0^t ds\ e^{(t-s)\Lambda}\mathcal{P}\Lambda e^{sQ\Lambda}. \tag{47}$$

## A2. *-Derivation of Eq.(49)-*

The second term of (47) gives

$$\int_0^t ds\, e^{(t-s)\Lambda}\mathcal{P}\Lambda R(s) = \int_0^t ds\, \langle\{\Lambda R(s)\}A^\dagger\rangle\langle AA^\dagger\rangle^{-1}A(t-s) \tag{A3}$$

which, together with the second term of (54), gives

$$\mathcal{M}(t) = -\langle\{\Lambda R(t)A^\dagger\}\rangle\langle AA^\dagger\rangle^{-1}. \tag{A4}$$

In order to prove $\langle\{\Lambda F\}G\rangle = -\langle F\{\Lambda G\}\rangle$, let us consider

$$\langle\{\Lambda F\}G\rangle = \lim_{t\to 0}\frac{1}{t}[\langle\{e^{t\Lambda}F\}G\rangle - \langle FG\rangle]$$
$$= -\lim_{t\to 0}\frac{1}{t}[\langle\{e^{-t\Lambda}F\}G\rangle - \langle FG\rangle] \tag{A5}$$

According to the Sinai-Ruelle-Bowen theorem of dynamical theory[12], there exists a unique measure $\mu(X)$ for a hyperbolic attractor $\mathcal{A}$ in phase space $X$ such that, for almost all initial states $X \in \mathcal{A}$, the long-time average can be writen

$$\langle f_1(t)f_2(0)\rangle \equiv \lim_{\tau\to\infty}\frac{1}{\tau}\int_0^\tau ds\ f_1(t+s)f_2(s)$$
$$= \int_{\mathcal{A}} f_1(t,X)f_2(0,X)\mu(dX). \tag{A6}$$

Using (A6), we have

$$\langle\{e^{-t\Lambda F}\}G\rangle = \int F(X(-t))G(X(0))\mu(dX(0))$$
$$= \int F(X(-t))G(X(0))\mu(dX(-t)), \tag{A7}$$

where we have $\mu(dX(0)) = \mu(X(-t))$ from the invariance of the probability measure $\mu(X)$. Setting $Y(0) = X(-t)$, we can write (A7) as

$$\int F(Y(0))G(Y(t))\mu(dY(0)) = \langle F\{e^{t\Lambda}G\}\rangle. \tag{A8}$$

Therefore inserting (A8) into (A5), we obtain

$$\langle\{\Lambda F\}G\rangle = -\lim_{t\to\infty}\frac{1}{t}[\langle F\{e^{t\Lambda}G\}\rangle - \langle FG\rangle] = -\langle F\{\Lambda G\}\rangle. \tag{A9}$$

(A4) can be written

$$\mathcal{M}(t) = \langle \widetilde{R}(t)\{\Lambda A^\dagger\}\rangle\langle AA^\dagger\rangle^{-1} \tag{A10}$$

Here, since $\langle \widetilde{R}(t)A^\dagger\rangle = 0$, $\Lambda A$ can be replaced by $\mathcal{Q}\Lambda A$, leads to

$$\mathcal{Q}\Lambda A = \mathcal{Q}\dot{A} = \widetilde{R}(0) \tag{A11}$$

which is inserted into (A10) to give (49)

$$\mathcal{M}(t) = \langle \widetilde{R}(t)\widetilde{R}^\dagger\rangle\langle AA^\dagger\rangle^{-1} \tag{49}$$